Materials Science in Semiconductor Processing 150 (2022) 106906

Contents lists available at ScienceDirect

Materials Science in Semiconductor Processing

journal homepage: www.elsevier.com/locate/mssp

Full length article

# Electronic properties and defect levels induced by *n*/*p*-type defect-complexes in Ge

E. Igumbor [a,*], O. Olaniyan [b], G.M. Dongho-Nguimdo [c], R.E. Mapasha [d], S. Ahmad [e], E. Omotoso [f], W.E. Meyer [d,*]

[a] Department of Mechanical Engineering Science, University of Johannesburg, Johannesburg, South Africa
[b] Department of Chemistry University of Free-State, 9300 Bloemfontein, South Africa
[c] Department of Electrical and Electronic Engineering, College of Technology, University of Buea, P.O. Box 63, Buea, Cameroon
[d] Department of Physics, University of Pretoria, Pretoria 0002, South Africa
[e] Department of Physics, College of Science. King Khalid University, P.O. BOX 9004 Abha, Saudi Arabia
[f] Department of Physics and Engineering Physics, Obafemi Awolowo University, Ile-Ife, Nigeria

ARTICLE INFO

*Keywords:*
Material modelling
Semiconductor
Electronic
Defect-complexes
Defect-level

ABSTRACT

Defect-complexes are point defects that significantly influence the geometric, optical, and electrical properties of materials. Defect-complexes are known to improve the electronic and electrical properties of Ge. Deep and shallow defect levels in Ge have been linked to defect-complexes formed by the double self-interstitials and rare earth atoms. Despite this breakthrough, several defect-complexes in Ge are not well understood; hence may pose as a challenge to the optimal performance of Ge based devices. In this study, we present the results of the hybrid density functional theory calculations of substitutional and interstitial defect-complexes ($B_{Ge}N_i$, $N_{Ge}B_i$, $Al_{Ge}P_i$, $P_{Ge}Al_i$, $Ga_{Ge}As_i$, $As_{Ge}Ga_i$, $In_{Ge}Sb_i$, and $Sb_{Ge}In_i$) in Ge. Their formation energies, electronic properties, defect-complex stability and induced defect levels in Ge were predicted. While the formation energies of the defect-complexes formed by the P and Al atoms were relatively low and energetically more favourable, those defect-complexes formed by the B and N atoms were the least energetically favourable. Except for the $B_{Ge}N_i$, all the defect-complexes significantly bound with energies lower than their formation energies. The $N_{Ge}B_i$ and $P_{Ge}Al_i$ essential donor levels were in the band gap of Ge. A shallow double acceptor defect level was found to be associated with the $Al_{Ge}P_i$, while the $In_{Ge}Sb_i$ induced a shallow double donor defect level. The electrical inactive defect-complexes were the $B_{Ge}N_i$, $Ga_{Ge}As_i$, $As_{Ge}Ga_i$ and $Sb_{Ge}In_i$. The results of this report are important, as they provide theoretical insight of the prediction of the *n*/*p*-type substitutional and interstitial defect-complexes in Ge.

## 1. Introduction

Germanium is an important material for applications in nanoelectronic, monolithic optoelectronic integration chips and metal-oxide-semiconductor field-effect transistors [1–4]. The important characteristics of Ge are its superior hole and electron carrier mobilities, low-dopant activation temperature and smaller band-gap (0.78 eV at 0 K) than that of the silicon [4–8]. Recently, there is a rising demand for *high-k* gate dielectric material; in addition to the amorphous oxides, Ge is being consider as alternative complementary source due to its high dielectric constant (e = 16) [9–12]. Ge is classified as an indirect bandgap semiconductor [6,13]; its conduction band minimum and valence band maximum are located at different **k**-vectors. Extensive theoretical studies of the engineering of the bandgap of Ge provide detailed descriptions of its evolution with doping and strain [1,14]. For instance, a *n*-type doping may be used to compensate the energy difference between the conduction and valence bands. This is achievable as the electrons coming from the activated *n*-type dopants shift the energy of the quasi-Fermi level higher towards the conduction band [15]. The study of point defects in semiconductor are increasing, due to the discovery that they improve the performance of their host, act as compensation centres, radiative and non radiative recombination centres [16,17].

Defects in materials cannot be completely avoided during implantations or diffusion processes [2,18,19]. Essentially, the understanding of defects in semiconductor is key to the comprehension of diffusion, migration and defect's control, which could lead to the productions of improved high quality devices [18–21]. Since the characteristic dimensions of devices is in a few nanometers, there is need to understand

* Corresponding authors.
*E-mail addresses:* elgumuk@gmail.com (E. Igumbor), wmeyer@up.ac.za (W.E. Meyer).

https://doi.org/10.1016/j.mssp.2022.106906
Received 9 February 2022; Received in revised form 7 June 2022; Accepted 17 June 2022
Available online 1 July 2022

fully the control of activities of *p*- and *n*-type dopants in semiconductor [22,23]. The *p*-type and *n*-type dopants are the main ingredient for the formation of highly efficient Ge-based *n*/*p*-type channel metal oxide semiconductor field effect transistors (MOSFET), which could be useful for advanced complementary metal-oxide semiconductors (CMOS) [2,3]. Due to the recent scaling scheme of CMOS devices in the last decades, efforts have been made to improve integrated circuit performance [15]. Reports have shown that if you want to manufacture a fast response device (such as Si diodes and transistors), it is required to decrease the lifetime of non-equilibrium charge carriers [24,25]. This could be achieved by the introduction of defects via implantation, electron irradiation and electron deposition, amongst other defect processes and characterization techniques [24–26]. Previously, studies of *n*-, *p*-type dopants and isovalent atoms, in germanium have been reported [2,27,28]. In a recent report [29], the insertion of P atom in germanium using $PF^+$ molecular implantation reveals its stability at 400 °C. The study further shows that the final junction depth could be adequately controlled by an implantation process, as this is essential for the formation of shallow junction Ge-based Fin-Field-Effect Transistor (FinFET) [29]. Device characterization in the presence of dopant are sometimes performed by deep level transient spectroscopy (DLTS) techniques [21], and it helps to understand how the *n*- or *p*-type impurities are controlled during implantations and irradiations processes. The *n*-type doping of Ge is reported to serve as a key parameter in recent breakthroughs of Si-compatible infrared emitting devices [30,31]. Co-doping of Ge by Sb/P and by using the Ga/P decomposition source produce smooth and heavily *n*-type doped Ge films epitaxially grown on Si(001) [15,32].

Defect-complexes may occur due to the damage caused by the displacement of lattices during radiation processes. Numerous studies that focused on the structural, electronic, optical and induced defect-levels of interstitial, vacancy and substitutions in germanium have been reported [2,27,33–36]. Nonetheless, very little is known about the dependence of the aforementioned properties due to defect-complexes in Ge. However, the study of defect-complexes of the GaN and Si semiconductors is gaining huge attention. For instance, the introduction of double and triple dopant defect-complexes in Mg–H co-doped GaN are suggested to act as compensations for the $Mg_{Ga}$ acceptor, which could influence the rate of the *p*-type conductivity [37]. The Mg–H defect-complex in GaN limits the *p*-type conductivity, induce non-radiative electron–hole recombination centre and give rise to a red and broad photoluminescence bands. The electrical deactivation and structural changes observed during an extended X-ray absorption fine structure analyses of arsenic-doped silicon have been ascribed to the defect-complex (V-$As_4$) which is energetically more favourable that the substitutional defect [38]. The formation of the recombination-active defect-complexes in Si acts as an avenue to mitigate the carrier-induced degradation in *p*-type silicon, most especially with the presence of the boron and oxygen impurities [39]. Defect-complexes in $PbTiO_3$ are responsible for the switching of the spontaneous ferroelectric polarization in the host material [40]. Recently, high irradiated Si was reported to produce strong bound carbon interstitial–carbon substitutional ($C_iC_s$), $C_iC_s(Si_i)$ and $C_iC_s(Si_i)_2$ defect-complexes [27]. Since the electro physical, mechanical, and optical properties of devices depend on a crystal and its defective structure, defect-complexes may as well alter these properties in Ge as reported for the case of Si [15,27,32]. The electrical properties of the radiation-induced interstitial boron and interstitial oxygen defect-complexes and their initial doping concentrations have been determined by exposing diodes to different resistivity values in Si [41]. The defect-complex $Al_iAl_{Ge}$ is reported to induce double donors in Ge at $E_V$ + 0.06 and $E_V$ + 0.12 [42] ($E_V$ is the energy of the valence band maximum) In addition to the traditional doping elements as discussed earlier, the group 4*f* rare-earth atoms have been used as dopants in several materials, as they improved the electronic and electrical properties of semiconductors [35,43,44]. The rare-earth doped GaN is reported to improve its optoelectronics and spintronics properties [45], which could be a potential candidate for quantum application. The influence of the rare-earth ion doped $Al_2O_3$ enhances the active integrated photonics of the host semiconductor [46]. Rare earth defect-complexes in Ge have been reported [35]. The Tm vacancy-complex in Ge induces shallow acceptor level at $E_V$ + 0.06 [47]. While the $Ce_{Ge}Ge_i$ induces deep donor level ($E_V$ + 0.49) with negative-U ordering, the $Pr_{Ge}Ge_i$ induces shallow defect level at $E_C$-0.01 eV [48] ($E_C$ is the energy of the conduction band minimum). The $Eu_{Ge}Ge_i$ defect level in Ge is located at an energy level of $E_V$ + 0.49 [48]. Despite the successes recorded in identifying deep or shallow defect-complexes induced in Ge, there are few reports on the *n*/*p*-type defect-complexes in Ge. In addition, report have shown that both the substitutional and interstitial doping of materials is responsible for the altering of the electronic and transport properties, lattice parameters, phase transitions, which could lead to the formation of various physiochemical properties that may influence the performance of the semiconductors [49]. In *h*-BN and *c*-BN, the self-interstitials $N_i$ and $B_i$ are low formation energies, which is in contrast to the vacancies $V_N$ and $V_B$(where the $V_N$ and $V_B$ are nitrogen and boron vacancy, respectively) [50]. Reports of the co-doping of semiconductors with *N* and B atoms and their influences on the electronic and electrical properties of their host are well known [51–55]. To the best of our knowledge, the possible combinations of the B interstitial or substitutional atom and *N* interstitial or substitution atom in Ge which may induce defect levels that could influence the electronic and electrical properties of the semiconductor is yet to be reported. The discussed research background on defect-complexes suggests that their influences on semiconductors are essentially needed to be understood to improve the realization of enhanced Ge based semiconductor devices. To this end, the understanding of the theoretical predictions of the formation of defect-complexes in Ge, especially those formed by the *n*/*p*-type interstitial and substitution is a major concern. Hence, this study provide a theoretical insight of the defect-complexes stability, the electronic and electrical properties of the *n*/*p*-type defects arising from the formation of the substitution and interstitial defect-complexes of group III–V atoms in Ge.

In this study, density functional theory with Heyd, Scuseria and Ernzerhof (HSE06) hybrid functional [56] was used to examined the charge state transition defect levels induced by the *n*/*p*-type defect-complexes in Ge. Furthermore, insights on the formation energies and the stability of the defect-complexes from the *n*/*p*-type substitution–interstitial in Ge were predicted. We showed that the introduction of the defect-complexes in Ge are essential as they altered the structural and electronic properties of Ge. The $N_{Ge}B_i$ and $Al_{Ge}P_i$ induced single deep defect level which act as recombination centre in Ge. The structure of this paper is organized as follows; in Section 2 we present the computational details. Section 3 focuses on the results and the discussion of the energetics and the stability of the defect-complexes, their electronic properties and defect levels induced in Ge. Finally, we present the conclusion of this report in Section 4.

## 2. Computational details

Hybrid density functional theory calculations were performed using the Vienna *ab-initio* Simulation Package (VASP) [57]. The chemically active valence electrons were separated from the core electrons using the projector-augmented wave (PAW) method [58]. While the $s^2p^1$ were used as the valence electrons for the *p*-type atoms, the $s^2p^3$ on the other hand, were used as the outer shell electrons for the *n*-type atoms. All calculations were performed using the HSE06 hybrid functional with the Perdew, Burke and Ernzerhof (PBE) [59]. The HSE06 approach is a combination of the PBE and the non-local Fock [56]. In all calculations, a mixing parameter of 25% (fraction of exact Hartree–Fock exchange) and 0.2 $Å^{-1}$ screening parameter were used. The mixing and screening parameters were sufficiently used to predict accurately the germanium band gap of 0.78 eV, which is in agreement with the

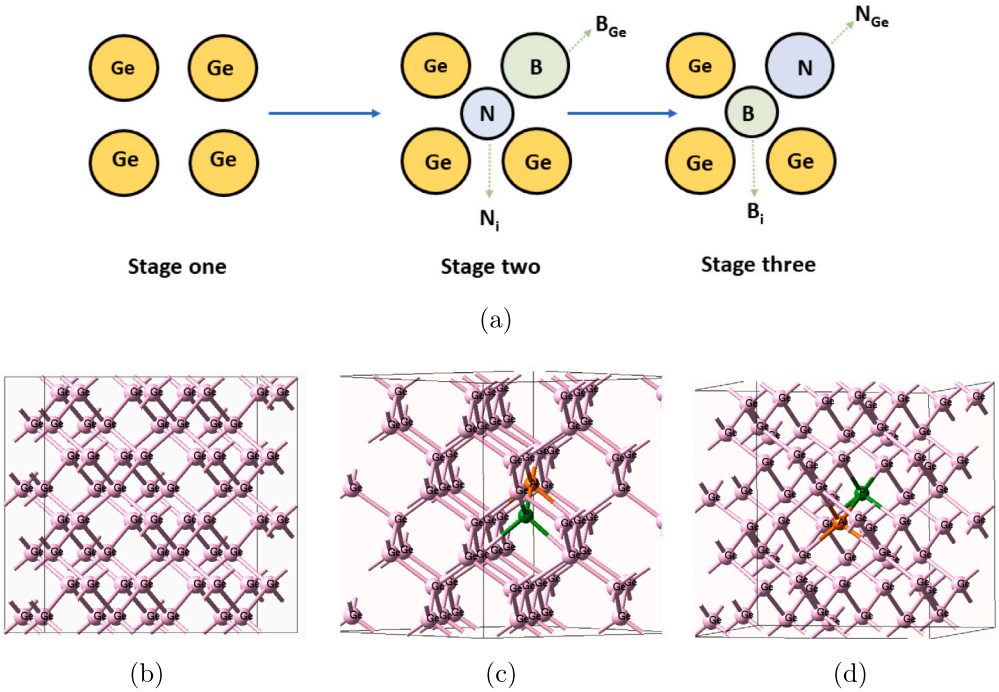


**Fig. 1.** (a) Schematic representation of the $n/p$-type impurities (top panel), crystal Ge (Stage one), substitution and interstitial defect-complexes, $B_{Ge}N_i$ (Stage two) and $N_{Ge}B_i$ (Stage three), (b) pristine Ge supercell (c) $Al_{Ge}P_i$ and (d) $P_{Ge}Al_i$.

experimental band gap [5]. For us to model the properties of $n/p$-types substitution and interstitial defect-complexes in Ge, we constructed a supercell of 64 atoms from the primitive unit cell. We optimized the supercell by sampling the Brillouin zone with a $2 \times 2 \times 2$ Monkhorst–Pack [60] k-points and energy cut-off of 400 eV. The forces acting on the atoms were less than 0.001 eV/Å and the minimum total energy difference convergence was set to $10^{-6}$ eV. Spin effect was accounted for in all calculations by the inclusion of spin orbit coupling. For the electronic properties calculations, i.e the partial density of states, a denser $16 \times 16 \times 16$ k-points mesh was used to integrate the Brillouin zone.

For us to determine the likelihood of incorporating $n/p$-type defect-complex in a Ge crystal, the defect formation energy was calculated. The formation energy $E^F(B_{Ge}N_i,q)$ of the $B_{Ge}N_i$ defect-complex in Ge, in its charge state $q$ as a function of the electron Fermi energy ($\varepsilon_F$) is given as [43,61]

$$E^F(B_{Ge}N_i,q) = E^{total}(B_{Ge}N_i,q) - E^{total}(Ge) + 2\mu_{Ge} - \mu_B - \mu_N + q[E_V + \varepsilon_F] + E^q_{FNV}. \quad (1)$$

The total energies of the $B_{Ge}N_i$ and the pristine supercell of Ge are represented by $E^{total}(B_{Ge}N_i,q)$ and $E^{total}(Ge)$, respectively. The $\mu_{Ge}$, $\mu_B$ and $\mu_N$ are the chemical potentials of the Ge, B and $N$ atoms, respectively. Whereas the criteria for calculating the chemical potential of the Ge atom and its value were taken from Ref. [62], the $\mu_B$ and $\mu_N$ were calculated as the total energy per number of impurity atom. When a supercell approach is adopted for the modelling of charged defects, errors due to finite-size effects and spurious interactions of charge states are bound to occur. The correction term $E^q_{FNV}$ according to the method of Ref. [63], was included to account for the errors that may arise as a result of the finite-size effects and defect-defect interactions.

The induced defect level in a semiconductor is theoretically obtained by calculating the thermodynamic charge state transition level. Charge state transition level denoted as $\epsilon(q/q')$, (where $q$ and $q'$ are two distinct charge states) is the point at which the formation energies of two charge states intersect in the band gap as the Fermi energy is varied from valence band maximum to the conduction band minimum. For instance, the $\epsilon(q/q')$ of the $B_{Ge}N_i$ defect-complex is calculated as [64]

$$\epsilon(q/q') = \frac{E^F(B_{Ge}N_i,q) - E^F(B_{Ge}N_i,q')}{q' - q}, \quad (2)$$

where the $E^F(B_{Ge}N_i,q)$ and $E^F(B_{Ge}N_i,q')$ are calculated at $\varepsilon_F = 0$

The defect-complex ($B_{Ge}N_i$) is an agglomeration of defects, which have the tendency to disintegrate into non interacting defects. The binding energy of the $B_{Ge}N_i$ provides information about the stability of such defect-complex. The binding energy $E_B$ of the $B_{Ge}N_i$ (in this reaction; $B_{Ge} + N_i \longrightarrow B_{Ge}N_i$) with formation energy $E^F(B_{Ge}N_i,0)$ in its neutral charge state is calculated as

$$E_B = E^{Form}(B_{Ge}) + E^{Form}(N_i) - E^F(B_{Ge}N_i,q), \quad (3)$$

where the $E^{Form}(B_{Ge})$ and $E^{Form}(N_i)$ are the formation energies of the B substitution in Ge ($B_{Ge}$) and N interstitial in Ge ($N_i$), respectively. Based on Eq. (3), a negative binding energy indicates that a cluster of defects is energetically unfavourable with respect to its constituent isolated non-interacting defect components. Hence, the defect-complexes could disintegrate into smaller fractions of non-interacting defects.

## 3. Results and discussion

The geometric properties of $n/p$-type defect-complexes in Ge were investigated. Fig. 1 displays a schematic diagram of $p$-type and $n$-type impurities and defect-complexes reported in this work. Due to the possibilities of point defects to exist as defect-complexes, the $p$-type and $n$-type impurities were introduced to Stage one (non defective system) as substitution and interstitial atoms (Stage two) or vice versa (Stage three) in Ge crystal as shown in Fig. 1(a). While Fig. 1(b) displays the relaxed geometric structure of the pristine Ge, the relaxed geometric structures of the $Al_{Ge}P_i$ and $P_{Ge}Al_i$ are respectively, shown in Figs. 1(d)–1(c). In a crystal solid, defects may exist in the form of single or multiple defects. For instance, the Ge self interstitials and vacancy have been reported [65–67]. Furthermore, as motivated in the introduction, defect-complexes have been identified in Ge [27,34,42]. In this report, the distribution of defects in the supercell were sampled, and the

formation energies of the $P_{Ge}Al_i$ and $Al_{Ge}P_i$ in different defect configurations were obtained. The above process allows us to know the defect configuration that is more energetically favourable, amidst the random distribution of defects in a periodic boundary supercell. Amongst the different defect configurations considered, two configurations were outstanding due to their low formation energies. Consequently, two possible defect configurations of the defect-complexes were examined for further assessment to ascertained the most energetically favourable. For the first configuration; the impurities atoms were isolated, i.e separated far apart from each other (not nearest neighbours). The second configuration; the impurity atoms were nearest neighbours. Under equilibrium conditions, the preliminary results suggest that when impurities atoms are separated far from each other, the formation energy is higher and less energetically favourable. For example, the formation energies of the $P_{Ge}Al_i$ and $Al_{Ge}P_i$ in the first configuration are 5.73 and 6.03 eV, respectively. Nevertheless, in the second configurations (when they are nearest neighbours), their formation energies are 5.13 and 5.40 eV, respectively. Furthermore, the stability of the defect-complexes analyses with respect to their binding energies shows that both the $P_{Ge}Al_i$ and $Al_{Ge}P_i$ are energetically stable in the two different configurations. The calculated binding energies of the $P_{Ge}Al_i$ and $Al_{Ge}P_i$ are 1.11 and 2.57 eV, respectively, when the defect atoms are far from each other. However, when the defect atoms are nearest neighbour, the binding energies of the $P_{Ge}Al_i$ and $Al_{Ge}P_i$ as shown in Table 1 are 1.71 and 3.32 eV, respectively. Therefore, the defect-configuration when the impurity atoms are nearest neighbours will be further consider in this study.

The relaxed bond length of the nearest neighbour Ge–Ge atoms in the non-defective Ge supercell has been reported to be 2.46 Å [42,68]. In this study, the introduction of external atoms distorted the pristine Ge crystal structure. For the $Al_{Ge}P_i$, $P_{Ge}Al_i$, $N_{Ge}B_i$ and $B_{Ge}N_i$, the relaxed bond lengths of the nearest neighbours Al–Ge, P–Ge, N–Ge and B–Ge atoms, respectively, reduced significantly by 0.07, 0.18, 0.42 and 0.35 Å, when compared with that of Ge–Ge bond length. This suggests that the introduction of the impurity atoms Al, P, *N* and B on Ge atom lattice sites caused the surrounding host atoms to relaxed inward. For the $As_{Ge}Ga_i$, $Ga_{Ge}As_i$, $Sb_{Ge}In_i$ and $In_{Ge}Sb_i$, the relaxed bond lengths of the nearest neighbour As–Ge, Ga–Ge, In–Ge and Sb–Ge are 2.48, 2.52, 2.59 and 2.70 Å, respectively. These relaxed bond lengths significantly increased by 0.02, 0.06, 0.13 and 0.24 Å, respectively, when compared with that of the relaxed nearest neighbour Ge–Ge bond length. The substitutional atoms of the $As_{Ge}Ga_i$, $Ga_{Ge}As_i$, $Sb_{Ge}In_i$ and $In_{Ge}Sb_i$ relaxed outward displacing the host atoms. The amount of strain induced due to external impurities in Ge crystal could lead to lattice distortions which may affect the energy of formation of the defects. Interstitial defects are known to cause large structural deformations [69,70]. The impact of an interstitial atom on the structural properties of a crystal structure could be ascertained via the analyses of phonon spectrum. Hence, the calculations of the dynamic stability of the *n*/*p*-type defect-complexes in Ge will form the focus of future study.

Defect in a solid crystal may modulates the electronic properties of the host material. In Ge, several defects have been proposed to impact its electronic properties including the band gap [28,42,48]. In this study, we have showed that the introduction of defects, induced mid gap states in Ge. Fig. 2 displays the plots of partial density of states (PDOS) of the *n*/*p*-type defect-complexes in Ge. The plot of the PDOS of the pristine Ge showed that its valence band maximum is close to the Fermi level. (see Fig. 2(a)). The $B_{Ge}N_i$ and $N_{Ge}B_i$ electronic states are lying on the Fermi level close to the valence band maximum. The different *p* orbital of the N, B and Ge atoms for the $B_{Ge}N_i$ and $N_{Ge}B_i$ are strongly hybridized. For the $B_{Ge}N_i$ as shown in the top panel of Fig. 2(b), the minority and majority spins are highly asymmetric, suggesting the possibility of spin polarization. The $N_{Ge}B_i$ has a small sharp peak lying close to the Fermi level from the valence band maximum. This sharp peak was induced by the *p* orbital of the *N* and B atoms and the *s* orbital of the *N* atom. The $Al_{Ge}P_i$ induced double sharp peaks

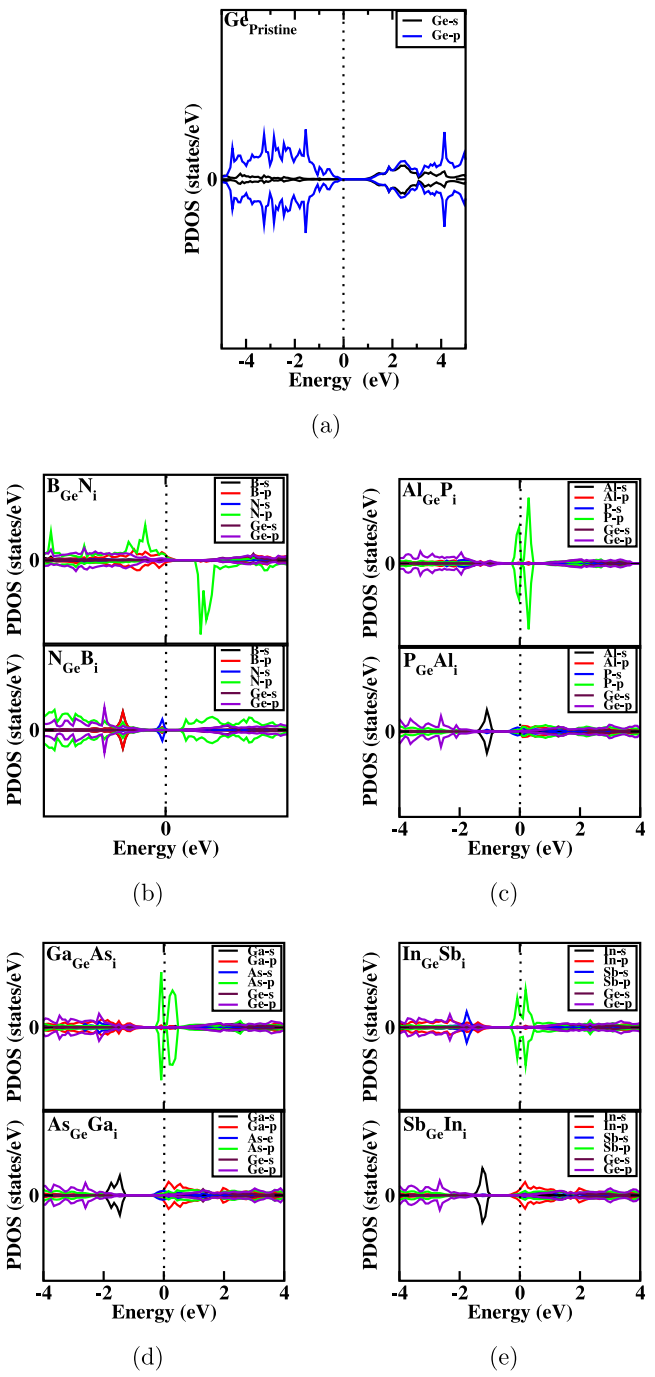


**Fig. 2.** Plots of partial density of states (PDOS) for the (a) Pristine Ge, (b) $B_{Ge}N_i$ and $N_{Ge}B_i$, (c) $Al_{Ge}P_i$ and $P_{Ge}Al_i$, (d) $Ga_{Ge}As_i$ and $As_{Ge}Ga_i$ and (e) $In_{Ge}Sb_i$ and $Sb_{Ge}In_i$. The red dash line represents the Fermi level, which is set to zero.

at the Fermi level. The $P_{Ge}Al_i$ exhibited an *n*-type semiconductivity as shown in the lower panel of Fig. 2(c). In addition, strong orbital hybridization was observed between the impurity atoms *p* orbital and that of Ge *p* orbital. The $In_{Ge}Sb_i$ and $Sb_{Ge}In_i$ induced mid gap states, which are mainly contributions from the *p* orbital of the external impurity atoms, Sb and In (see Fig. 2(e)). For the $As_{Ge}Ga_i$ and $Ga_{Ge}As_i$, their Fermi levels are lying in the conduction band minimum. The mid gap states induced by the $Sb_{Ge}In_i$ are relatively small peak, whereas those induced by the $In_iSb_{Ge}$ are broad. The $In_{Ge}Sb_i$ and $In_iSb_{Ge}$ are excellent *n*-type semiconductors.

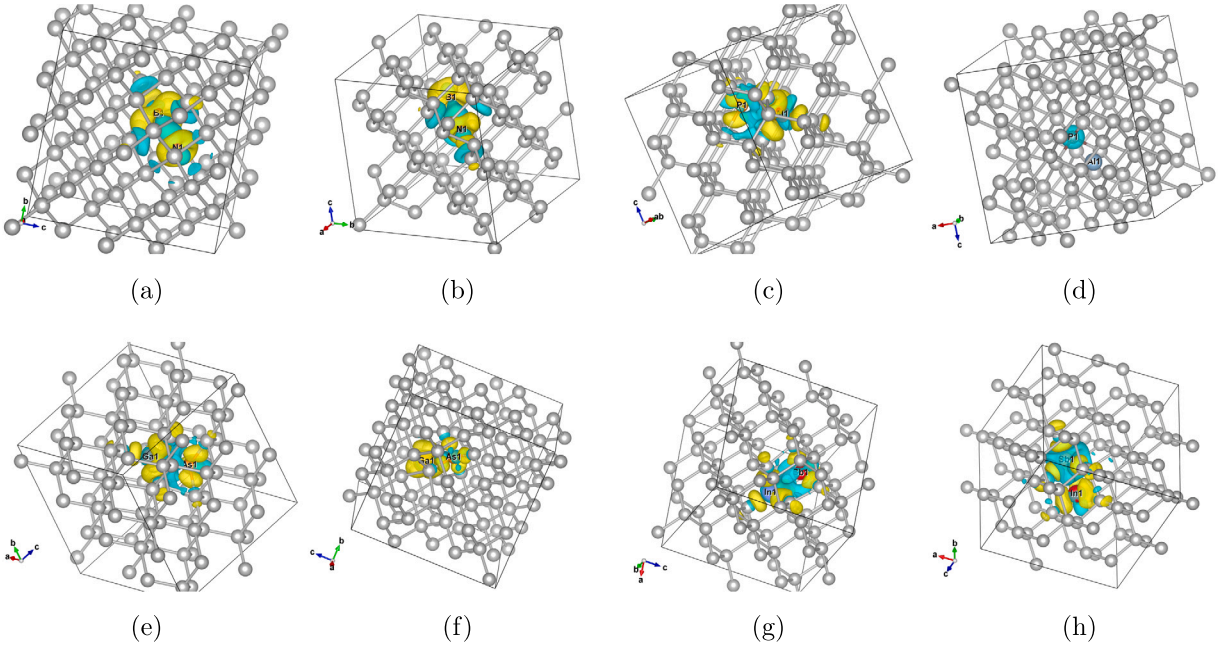


**Fig. 3.** Plots of isosurface of charge density difference for the (a) $B_{Ge}N_i$, (b) $N_{Ge}B_i$, (c) $Al_{Ge}P_i$, (d) $P_{Ge}Al_i$, (e) $Ga_{Ge}As_i$, (f) $As_{Ge}Ga_i$, (g) $In_{Ge}Sb_i$ and (h) $Sb_{Ge}In_i$. The grey atoms are Ge.

The planar average charge density difference is also important for describing the charge transition of a system [71–73]. In this report, the electron charge transfer analyses were performed to describe the charge density transitions. From the Bader charge analysis results, the charge transfer between impurity and the neighbouring Ge atoms were obtained and the plots of the isosurface of charge density difference are shown in Fig. 3. For the $B_{Ge}N_i$, $N_{Ge}B_i$, $Al_{Ge}P_i$, $P_{Ge}Al_i$, $Ga_{Ge}As_i$ and $As_{Ge}Ga_i$, the charge ($e^-$) on the interstitial(substitution) atoms are −1.75(1.00), −0.33(−1.19), −0.80(1.60), 1.30(−0.81), −0.18(0.27) and 0.35(−0.40), respectively. For the $B_{Ge}N_i$ and $N_{Ge}B_i$, the $N$ atom either in the substitutional or interstitial position, gained the largest electron charge transfer as seen in the charge density difference plots in Fig. 3. The excess charge distribution on the $N$ atom is gained from the nearest neighbour B and the surrounding Ge atoms. The P atoms in both $Al_{Ge}P_i$ and $P_{Ge}Al_i$ defect configurations released as much as 0.80 electron charge. The Al atom accumulated significant electron charge within the range of 1.30–1.60 $e^-$ from its neighbouring Ge and nearest neighbour P atoms. For the $In_{Ge}Sb_i$, the charge transfer ($e^-$) on the interstitial(substitution) atom is 0.00(0.40). The Sb atom retained its universal charge status whereas the In atom released 0.40 $e^-$ to its nearest neighbour Ge atoms. Also, for the $Sb_{Ge}In_i$, the electron charge on the Sb atom is −0.25 $e^-$, whereas that of the In atom is −0.30 $e^-$. This suggests that both atoms released electrons to the neighbouring Ge atoms. In general, charge transfer analyses results showed that the electron charge transfer is pronounced between the interstitial and substitutional atoms (see the plots of the isosurface of charge density difference shown in Fig. 3). All the $n$-type atoms received excess electron charges from their neighbouring atoms while the $p$-type atoms gave out electron charges. Furthermore, charge compensation was observed between the $n/p$-type defect-complexes in Ge.

The results of the calculation of $n/p$-type defect-complexes formation energies in their different configurations provide theoretical insight on the possibility of such defects to form in the host material. Table 1 lists the energies of formation and the binding energies of the neutral charge state of the $n/p$-type substitution and interstitial defect-complexes in Ge. While the $B_{Ge}N_i$ and $N_{Ge}B_i$ defect-complexes formation energies are relatively high, defect-complexes formed by the P and Al atoms are the most stable with formation energies within 5.13–5.40 eV. Careful assessment of the formation energies of defect-complexes, suggest that the $P_{Ge}Al_i$ has the lowest formation energy, whereas the $B_{Ge}N_i$ has the highest formation energy. This validates the tendency of the $P_{Ge}Al_i$ to form in Ge during defect processes.

**Table 1**
The formation ($E^F$) and binding energies ($E_B$) all in eV of $n$-type (N, P, As, and Sb) and $p$-type (B, Al, Ga and In) substitution and interstitial complexes in Ge at $\epsilon_F = 0$. According to Eq. (3), all positive and negative $E_B$ are stable and unstable defect-complexes, respectively.

| Defect | Reaction | $E^F$ | $E_B$ |
|---|---|---|---|
| $B_{Ge}N_i$ | $B_{Ge}$+ $N_i$ | 11.90 | −1.12 |
| $N_{Ge}B_i$ | $N_{Ge}$+ $B_i$ | 11.72 | 0.47 |
| $Al_{Ge}P_i$ | $Al_{Ge}$+ $P_i$ | 5.40 | 3.20 |
| $P_{Ge}Al_i$ | $P_{Ge}$+ $Al_i$ | 5.13 | 1.71 |
| $Ga_{Ge}As_i$ | $Ga_{Ge}$+ $As_i$ | 6.37 | 3.18 |
| $As_{Ge}Ga_i$ | $As_{Ge}$+ $Ga_i$ | 5.83 | 3.97 |
| $In_{Ge}Sb_i$ | $In_{Ge}$+ $Sb_i$ | 9.07 | 2.76 |
| $Sb_{Ge}In_i$ | $Sb_{Ge}$+ $In_i$ | 8.64 | 1.03 |

There is a possibility of defect-complexes to decompose into non interacting defects. For us to ascertain these possibilities, the binding energies of defect-complexes were calculated. The $N_{Ge}B_i$ is stable with a binding energy of 0.47 eV. The $Al_{Ge}P_i$, $Ga_{Ge}As_i$ and $As_{Ge}Ga_i$ are the most strongly bounded defect-complexes, with binding energies of 3.20, 3.18 and 3.97 eV, respectively. The binding energy results strongly depict that the $Al_{Ge}P_i$ and $In_{Ge}Sb_i$ defect-complexes are more stable when the substitutional impurity is a $p$-type atom. The $N_{Ge}B_i$ and $As_{Ge}Ga_i$ on the other hand, are strongly bounded when the interstitial atom is a trivalent impurity. The $B_{Ge}N_i$ is not stable in its neutral charge state. This suggests that during implantation, the $B_{Ge}N_i$ could dissociate into non interacting $B_{Ge}$ and $N_i$ constituent defects with energy lower that 11.90 eV.

Defect levels induced by the $n/p$-type defect-complexes in Ge were investigated. Table 2 lists the charge state transition energy levels and Fig. 4 shows the plot of the charge state as a function of the Fermi energy. All defect-complexes induced defect levels except for the $B_{Ge}N_i$, $Sb_{Ge}In_i$, $Ga_{Ge}As_i$ and $As_{Ge}Ga_i$. In the absence of electrically active defect levels, the $B_{Ge}N_i$ and $Sb_{Ge}In_i$ charge states of −2 and

**Table 2**
The charge state transition ($\varepsilon(q/q')$) energy levels above the VBM in eV induced by $n/p$-type substitution–interstitial defect-complexes in Ge.

| Defect | (+2/ + 1) | (+1/0) | (0/ − 1) | (−1/ − 2) |
|---|---|---|---|---|
| $N_{Ge}B_i$ | – | 0.25 | 0.57 | – |
| $Al_{Ge}P_i$ | 0.20 | 0.35 | 0.50 | 0.66 |
| $P_{Ge}Al_i$ | 0.61 | – | – | – |
| $In_{Ge}Sb_i$ | 0.68 | – | – | – |

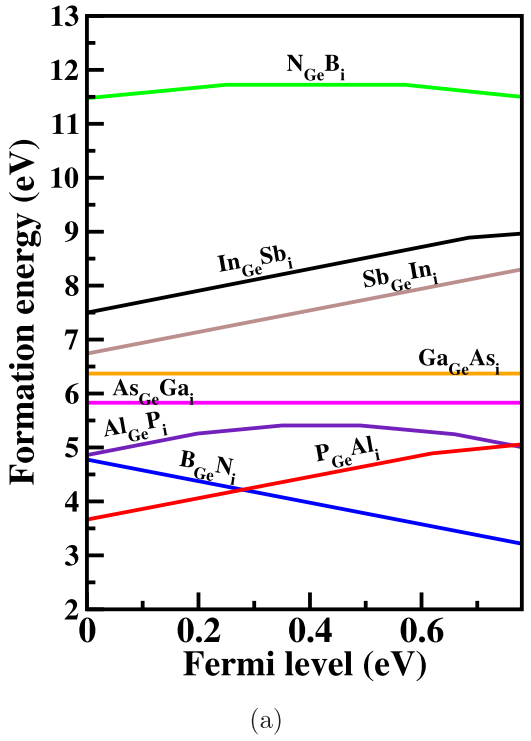


**Fig. 4.** Plots of formation energies as a function of the Fermi level for interstitial–substitutions defect-complexes in Ge. The slope of each plot corresponds to the charge state transition level.

+2, respectively, are thermodynamically stable for all Fermi energies. This suggests that the $B_{Ge}N_i$ behaves as a donor and the $N_{Ge}B_i$ exhibits acceptor characteristics. The $Ga_{Ge}As_i$ and $As_{Ge}Ga_i$ on the other hand, are charge state thermodynamically stable in their neutral charge state. The neutral charge state primarily dominates the band gap of Ge for all Fermi energies. Defect may induce energy levels that are not close to either the VBM or the CBM. Such defect levels are deep and have high ionization energies which could retard the contribution of free charge carriers. Also, defect levels close to the valence band edge or the conduction band minimum are shallow defects with energies less than or in the order of 3 $k_{BT}$. The $P_{Ge}Al_i$ is a deep donor and the $In_{Ge}Sb_i$ induces a shallow single donor level close to the conduction band minimum. For the $P_{Ge}Al_i$, the +1 charge state principally dominates the band gap up to an energy level of 0.61 eV, whereas for the $In_{Ge}Sb_i$, its (+1/0) energy level is located at $E_C$−0.10 eV. The induced defect level of the (+1/0) for the $In_{Ge}Sb_i$ is arguably an important defect level, which could ionized at room temperature (300 K) and improved the donation of electrons to the conduction band. The $Al_{Ge}P_i$ induced four defect levels in Ge: the (+2/+1), (+1/0), (0/−1) and (−1/−2). Whereas the energy level of the (+2/+1) is $E_V$ + 0.20 eV, that of the (+1/0) as the Fermi energy is varied from the valence band maximum to the conduction band minimum is $E_V$ + 0.35 eV. When a defect induces energy level in the band gap of a semiconductor, with its energy located at the middle or deep from both the VBM and CBM, such deep defect is known to act as a recombination centre. Hence, the (+1/0) defect level of the $Al_{Ge}P_i$ is deep, and acts as a recombination centre thereby reducing the carriers lifetime. Furthermore, the $Al_{Ge}P_i$ acceptors, i.e (0/−1) and (−1/−2), are deep and lying at $E_C$−0.38 (which has the tendency to act as a recombination centre) and $E_C$-0.12 eV, respectively. The $N_{Ge}B_i$ defect levels are possible deep traps in the band gap of Ge. The single acceptor and donor defect levels of the $N_{Ge}B_i$ are located at $E_V$ + 0.25 eV and $E_C$ − 0.21 eV, respectively. The $N_{Ge}B_i$ formed with a high energy, suggesting the possibilities of its defect levels to exist during implantations at energy above 10.00 eV. The presence of deep defect levels in the $N_{Ge}B_i$, $Al_{Ge}P_i$ and $P_{Ge}Al_i$, suggest the possibility that the host and impurity atoms formed weak bond due to high level of strain. This possibility further produce large lattice distortion which could probably enhance defect precipitation.

## 4. Conclusion

Density functional theory calculations of $n/p$-type interstitial and substitutional defect-complexes in Ge were studied using the HSE06 hybrid functional. The formation and stability of the $B_{Ge}N_i$, $N_{Ge}B_i$, $Al_{Ge}P_i$, $P_{Ge}Al_i$, $Ga_{Ge}As_i$, $As_{Ge}Ge_i$, $In_{Ge}Sb_i$ and $Sb_{Ge}In_i$ defect-complexes were established. The electronic properties and defect levels induced in Ge by the aforementioned defects were predicted. Under equilibrium conditions, the $P_{Ge}Al_i$ is the energetically most favourable, whereas the $B_{Ge}N_i$ is the least energetically favourable. Except for the $B_{Ge}N_i$, all defect-complexes considered in this study were stable with respect to their binding energies, hence dissociation will only occur at expense of energy relatively higher than their formation energies. Defect levels analyses showed that the $B_{Ge}N_i$, $Ga_{Ge}As_i$, $As_{Ge}Ga_i$ and $Sb_{Ge}In_i$ are electrically inactive. Furthermore, while the $In_{Ge}Sb_i$ and $P_{Ge}Al_i$ induced single donor, the $Al_{Ge}P_i$ and $N_{Ge}B_i$ induced single deep defect levels which act as recombination centres. This study of the defect-complexes provides new insights on the theoretical prediction of point defects in Ge. In addition, the unique response to the incorporation of $n/p$-type interstitial and substitutional defect-complexes which critically influence the properties of Ge will provide essential information, that are useful during the implantation processes in Ge and Ge-based device engineering.

## CRediT authorship contribution statement

**E. Igumbor:** Writing – review & editing, Writing – original draft, Visualization, Validation, Methodology, Investigation, Formal analysis, Data curation, Conceptualization. **O. Olaniyan:** Writing – review & editing, Visualization, Validation. **G.M. Dongho-Nguimdo:** Writing – review & editing. **R.E. Mapasha:** Writing – review & editing, Writing – original draft, Visualization, Validation, Supervision, Methodology. **S. Ahmad:** Writing – review & editing, Validation. **E. Omotoso:** Writing – review & editing, Writing – original draft. **W.E. Meyer:** Supervision, Software.

## Declaration of competing interest

The authors declare that they have no known competing financial interests or personal relationships that could have appeared to influence the work reported in this paper.

## Data availability

Data will be made available on request.

## Acknowledgements

Sohail Ahmad extends his appreciation to the Deanship of Scientific Research at King Khalid University, Saudi Arabia for financial support through research groups program under grant number (R.G.P. 2/139/43). This work is based on the research supported partly by National Research foundation (NRF) of South Africa (Grant specific unique reference number 98961). The opinions, findings and conclusion expressed are those of the authors and the NRF accepts no liability whatsoever in this regard. Emmanuel Igumbor is grateful to the University of Johannesburg for financial support. The authors are grateful to the Center for High Performance Computing (CHPC) Cape Town South Africa for providing computational resources.

## References

[1] Q. Wei, J. Song, C. Zhou, W. Bao, Y. Miao, H. Hu, H. Zhang, B. Wang, Mater. Express 7 (5) (2017) 369–379.
[2] E. Sgourou, Y. Panayiotatos, R. Vovk, N. Kuganathan, A. Chroneos, Appl. Sci. 9 (12) (2019) 2454.
[3] Y. Li, R. Zhang, Appl. Phys. Lett. 114 (13) (2019) 132101.
[4] D. Brunco, B. De Jaeger, G. Eneman, J. Mitard, G. Hellings, A. Satta, V. Terzieva, L. Souriau, F. Leys, G. Pourtois, et al., J. Electrochem. Soc. 155 (7) (2008) H552.
[5] F.J. Morin, J.P. Maita, Phys. Rev. 94 (1954) 1525–1529.
[6] K. Moto, R. Yoshimine, T. Suemasu, K. Toko, Sci. Rep. 8 (1) (2018) 1–7.
[7] A. Nayfeh, C.O. Chui, T. Yonehara, K.C. Saraswat, IEEE Electron Device Lett. 26 (5) (2005) 311–313.
[8] L. Lee, E.A. Fitzgerald, T. Bulsara, Mayank, T. Currie, A. Lochtefeld, J. Appl. Phys. 97 (1) (2005) 011101.
[9] C. Yuan, P. Darmawan, Y. Setiawan, P. Lee, Europhys. Lett. 74 (1) (2006) 177.
[10] C.H. Lee, J.Y. Yang, J. Heo, G. Yoo, IEEE J. Electron Devices Soc. 9 (2021) 295–299.
[11] C. Emminger, R. Carrasco, N. Samarasingha, F. Abadizaman, S. Zollner, 2018 IEEE Photonics Society Summer Topical Meeting Series (SUM), IEEE, 2018, pp. 149–150.
[12] Y. Kamata, Mater. Today 11 (1–2) (2008) 30–38.
[13] M. El Kurdi, M. Prost, A. Ghrib, S. Sauvage, X. Checoury, G. Beaudoin, I. Sagnes, G. Picardi, R. Ossikovski, P. Boucaud, ACS Photonics 3 (3) (2016) 443–448.
[14] Q. Fan, C. Chai, Q. Wei, Q. Yang, P. Zhou, M. Xing, Y. Yang, Mater. Sci. Semicond. Process. 43 (2016) 187–195.
[15] M. Zrir, B. Alek, A. Hussein, S. Shaker, J. Appl. Phys. 123 (13) (2018) 133102.
[16] J.-H. Yang, L. Shi, L.-W. Wang, S.-H. Wei, Sci. Rep. 6 (2016) 21712.
[17] Z. Xie, Y. Sui, J. Buckeridge, C.R.A. Catlow, T.W. Keal, P. Sherwood, A. Walsh, M.R. Farrow, D.O. Scanlon, S.M. Woodley, et al., J. Phys. D: Appl. Phys. 52 (33) (2019) 335104.
[18] M.A. Luong, E. Robin, N. Pauc, P. Gentile, M. Sistani, A. Lugstein, M. Spies, B. Fernandez, M.I. Den Hertog, ACS Appl. Nano Mater. 3 (2) (2020) 1891–1899.
[19] S. Kumari, A. Dutta, Materialia (2020) 100666.
[20] T. Luong, V. Le Thanh, A. Ghrib, M. El Kurdi, P. Boucaud, Phys. Scr. 94 (8) (2019) 085803.
[21] V. Gora, F. Auret, H. Danga, S. Tunhuma, C. Nyamhere, E. Igumbor, A. Chawanda, Mater. Sci. Eng. B 247 (2019) 114370.
[22] P. Reiser, F.S. Benneckendorf, M.-M. Barf, L. Müller, R. Bäuerle, S. Hillebrandt, S. Beck, R. Lovrincic, E. Mankel, J. Freudenberg, et al., Chem. Mater. 31 (11) (2019) 4213–4221.
[23] S. Lan, Y. Yan, H. Yang, G. Zhang, Y. Ye, F. Li, H. Chen, T. Guo, J. Mater. Chem. C 7 (15) (2019) 4543–4550.
[24] J. Liu, J. Wang, Y. Liu, G. Yan, W. Rui, R. Wang, Spectrosc. Lett. 52 (8) (2019) 441–446.
[25] S. Ke, J. Zhou, S. He, X. Ou, C. Li, S. Chen, Semicond. Sci. Technol. 35 (3) (2020) 035012.
[26] Y.-J. Chen, H.-H. Liao, B.-Y. Tsui, Y.-J. Lee, C.-J. Wang, P.-J. Sung, Vacuum (2020) 109528.
[27] S.-R. Christopoulos, E. Sgourou, R. Vovk, A. Chroneos, C. Londos, J. Mater. Sci., Mater. Electron. 29 (5) (2018) 4261–4265.
[28] E. Igumbor, G. Dongho-Nguimdo, R.E. Mapasha, W.E. Meyer, J. Mater. Sci. 54 (15) (2019) 10798–10808.
[29] J. Liu, G. Wang, J. Li, Z. Kong, H.H. Radamson, J. Mater. Sci., Mater. Electron. 31 (1) (2020) 161–166.
[30] S. Ray, S. Maikap, W. Banerjee, S. Das, J. Phys. D: Appl. Phys. 46 (15) (2013) 153001.
[31] H. Tseng, K. Wu, H. Li, V. Mashanov, H. Cheng, G. Sun, R. Soref, Appl. Phys. Lett. 102 (18) (2013) 182106.
[32] T. Luong, A. Ghrib, M. Dau, M. Zrir, M. Stoffel, V. Le Thanh, R. Daineche, T. Le, V. Heresanu, O. Abbes, et al., Thin Solid Films 557 (2014) 70–75.
[33] L. Khirunenko, M. Sosnin, A. Duvanskii, N. Abrosimov, H. Riemann, J. Appl. Phys. 123 (16) (2018) 161595.
[34] E. Igumbor, E. Omotoso, S.M. Tunhuma, H.T. Danga, W.E. Meyer, Nucl. Instrum. Methods Phys. Res. B 409 (2017) 31–35.
[35] E. Igumbor, W. Meyer, Mater. Sci. Semicond. Process. 43 (2016) 129–133.
[36] A. Chroneos, Semicond. Sci. Technol. 26 (9) (2011) 095017.
[37] M. Huang, H. Li, S. Chen, Phys. Status Solidi (A) 218 (7) (2021) 2000723.
[38] K. Pandey, A. Erbil, G. Cargill III, R. Boehme, D. Vanderbilt, Phys. Rev. Lett. 61 (11) (1988) 1282.
[39] B.J. Hallam, M.D. Abbott, N. Nampalli, P.G. Hamer, S.R. Wenham, IEEE J. Photovolt. 6 (1) (2015) 92–99.
[40] P. Marton, C. Elsässer, Phys. Rev. B 83 (2) (2011) 020106.
[41] C. Liao, E. Fretwurst, E. Garutti, J. Schwandt, M. Moll, A. Himmerlich, Y. Gurimskaya, I. Pintilie, A. Nitescu, Z. Li, et al., IEEE Trans. Nucl. Sci. 69 (3) (2022) 576–586.
[42] E. Igumbor, R.E. Mapasha, W.E. Meyer, J. Electron. Mater. (2016) 1–8.
[43] E. Igumbor, R.C. Andrew, W.E. Meyer, J. Electron. Mater. 46 (2) (2017) 1022–1029.
[44] L. Oliveira, J. Cortés, B. Caldeira, T. Strusch, U. Wiedwald, A. Simoes, Ceram. Int. 47 (15) (2021) 20768–20780.
[45] K. Hoang, 2022, arXiv preprint arXiv:2201.03651.
[46] C. Guillaume, J. Frieiro, O. Blázquez, C. Labbe, J. López-Vidrier, B. Garrido, S. Hernández, B. Liu, L. Khomenkova, C. Frilay, et al., Appl. Surf. Sci. 556 (2021) 149754.
[47] E. Igumbor, R.E. Mapasha, R. Andrew, W.E. Meyer, Comput. Condens. Matter 8 (2016) 31–35.
[48] E. Igumbor, E. Omotoso, H.T. Danga, S.M. Tunhuma, W.E. Meyer, Nucl. Instrum. Methods Phys. Res. B 409 (2017) 9–13.
[49] T. Chen, C. Foo, S.C.E. Tsang, Chem. Sci. 12 (2) (2021) 517–532.
[50] W. Orellana, H. Chacham, Phys. Rev. B 63 (12) (2001) 125205.
[51] D. Sahu, A. Palai, N.R. Panda, J. Mater. Sci., Mater. Electron. (2021) 1–15.
[52] D. Jana, C.-L. Sun, L.-C. Chen, K.-H. Chen, Prog. Mater. Sci. 58 (5) (2013) 565–635.
[53] E.H. Åhlgren, J. Kotakoski, A. Krasheninnikov, Phys. Rev. B 83 (11) (2011) 115424.
[54] S. Azevedo, J.R. Kaschny, C.M. de Castilho, F. de Brito Mota, Nanotechnology 18 (49) (2007) 495707.
[55] V. Gubanov, Z. Lu, B.M. Klein, C. Fong, Phys. Rev. B 53 (8) (1996) 4377.
[56] J. Heyd, G.E. Scuseria, M. Ernzerhof, J. Chem. Phys. 118 (18) (2003) 8207–8215.
[57] G. Kresse, J. Furthmüller, Phys. Rev. B 54 (1996) 11169–11186.
[58] P.E. Blochl, Phys. Rev. B 50 (1994) 17953–17979.
[59] J.P. Perdew, K. Burke, M. Ernzerhof, Phys. Rev. Lett. 77 (1996) 3865–3868.
[60] H.J. Monkhorst, J.D. Pack, Phys. Rev. B 13 (1976) 5188–5192.
[61] S.B. Zhang, J.E. Northrup, Phys. Rev. Lett. 67 (1991) 2339–2342.
[62] E. Igumbor, C. Ouma, G. Webb, W. Meyer, Physica B 480 (2016) 191–195.
[63] Y. Kumagai, F. Oba, Phys. Rev. B 89 (2014) 195205.
[64] C. Freysoldt, B. Grabowski, T. Hickel, J. Neugebauer, G. Kresse, A. Janotti, C.G. Van de Walle, Rev. Modern Phys. 86 (2014) 253–305.
[65] A. Carvalho, R. Jones, C. Janke, J.P. Goss, P.R. Briddon, J. Coutinho, S. Öberg, Phys. Rev. Lett. 99 (2007) 175502.
[66] P. Śpiewak, J. Vanhellemont, K. Sueoka, K. Kurzydłowski, I. Romandic, Mater. Sci. Semicond. Process. 11 (5) (2008) 328–331.
[67] C. Janke, R. Jones, S. Öberg, P.R. Briddon, Phys. Rev. B 75 (2007) 195–208.
[68] A. Chroneos, B.P. Uberuaga, R.W. Grimes, J. Appl. Phys. 102 (8) (2007) 083707.
[69] Y. Wu, C. He, W. Zhang, ACS Appl. Mater. Interfaces 13 (40) (2021) 47520–47529.
[70] H. Fiedler, F. Fuchs, J. Leveneur, M. Nancarrow, D.R. Mitchell, J. Schuster, J. Kennedy, Adv. Electron. Mater. 7 (8) (2021) 2100358.
[71] Q. Zhao, Y. Guo, Y. Zhou, Z. Yao, Z. Ren, J. Bai, X. Xu, Nanoscale 10 (7) (2018) 3547–3555.
[72] W. Zhang, Y. Yin, C. He, J. Phys. Chem. Lett. 12 (21) (2021) 5064–5075.
[73] C. He, Y. Liang, W. Zhang, Appl. Surf. Sci. 553 (2021) 149550.